SLAC−PUB−13333

# On Projecting Discretized Electromagnetic Fields with Unstructured Grids

Lie-Quan Lee*, Arno Candel, Andrea Kabel, and Zenghai Li
Stanford Linear Accelerator Center, 2575 Sand Hill Road, Menlo Park, CA 94025

***Abstract*—A new method for projecting discretized electromagnetic fields on one unstructured grid to another grid is presented in this paper. Two examples are used for studying the errors of different projection methods. The analysis shows that the new method is very effective on balancing both the error of the electric field and that of the magnetic field (or curl of the electric field).**

## I. Introduction

In performing eigen-mode analysis of electromagnetic cavities, the grid-based multi-level method [1], [2] is extremely useful for solving a highly-indefinite shifted linear system. In the multi-grid method, there exists multiple meshes generated with different mesh sizes. discretized vectors have to be projected from one mesh to another in the processes of restriction and prolongation. Similarly, in performing time-domain analysis of the cavities with an eigen-mode as ambient load, the eigen-mode that is often computed with a different mesh needs to be projected to the mesh used for time-domain analysis. The projected eigenvector can also serve as a initial guess for the eigenvector solution of the dense mesh in eigenpair refinement.

One way of projecting a discretized vector on one mesh to another is to use interpolation with basis functions on the meshes. For electromagnetics, the simple interpolation is good at controling the error of electric fields but it failed to control that of the magnetic field (o the curl of the electric field). In this paper, a new projection method that has better error control of both electric and magnetic fields is proposed. The outline the rest of the paper is as follows. First, a brief introduction of eigen-mode analysis is given. Then the new projection method is presented and its physical meaning is discussed. Two examples are given to show the errors of the new projection method. Finally, a summary of this work is given.

## II. Eigen-Mode Analysis

In analyzing eigen-modes of electromagnetic cavities, the governing Maxwell's equations can be simplified to the following harmonic vector wave equation:

$$\nabla \times \left( \frac{1}{\mu} \nabla \times \overrightarrow{\mathbf{E}} \right) - \varepsilon k^2 \overrightarrow{\mathbf{E}} = 0 \tag{1}$$

where $\varepsilon$ and $\mu$ are the relative electric permittivity and magnetic permeability and $k$ the angular wavenumber. With finite-element discretization using tangentially-continuous Nedelec basis functions [3],

$$\overrightarrow{\mathbf{E}} = \sum_i x_i \overrightarrow{\mathbf{N}}_i \tag{2}$$

the above equation becomes a generalized eigenvalue problem for a cavity with perfectly conducting cavity wall:

$$\mathbf{K}\mathbf{x} = \mathbf{M}\mathbf{x}k^2. \tag{3}$$

where the matrices $\mathbf{K}$ and $\mathbf{M}$ are

$$\mathbf{K}_{ij} = \left( \frac{1}{\mu} \nabla \times \overrightarrow{\mathbf{N}}_i, \nabla \times \overrightarrow{\mathbf{N}}_j \right), \quad and \tag{4}$$

$$\mathbf{M}_{ij} = \left( \varepsilon \overrightarrow{\mathbf{N}}_i, \overrightarrow{\mathbf{N}}_j \right). \tag{5}$$

Here we denote $(\overrightarrow{\mathbf{X}}, \overrightarrow{\mathbf{Y}})$ to be an inner product, which is the integral over the domain $\int_\Omega \overrightarrow{\mathbf{X}} \cdot \overrightarrow{\mathbf{Y}} \, d\Omega$. Note that matrix $\mathbf{M}$ is symmetric positive definite and matrix $\mathbf{K}$ is symmetric positive semi-definite with a large null space. Once the eigenvalue problem is solved, the electric field $\overrightarrow{\mathbf{E}}$ is recovered with Eq(2) while the magnetic field $\overrightarrow{\mathbf{B}}$ is computed with

$$\overrightarrow{\mathbf{B}} = -jkc \sum_i x_i \nabla \times \overrightarrow{\mathbf{N}}_i \tag{6}$$

where $j$ is the square root of $-1$ and $c$ the speed of light.

A shift-and-invert transformation as follows is often applied to Eq (3) in the process of solving the above eigenvalue problem since the interior eigenvalues are of the interest in the accelerator cavity modeling.

$$\frac{1}{k^2 - \sigma} \mathbf{x} = (\mathbf{K} - \sigma \mathbf{M})^{-1} \mathbf{M}\mathbf{x} \tag{7}$$

where $\sigma$ is a prescribed shift close to the eigenvalues of the interest. The above spectral transformation requires a solution of a highly indefinite linear system in every eigenvalue iteration, which is notoriously difficult to solve with iterative methods.

$$(\mathbf{K} - \sigma \mathbf{M}) \, \mathbf{y} = \mathbf{M}\mathbf{b} \tag{8}$$

To solve the shifted linear system Eq(8), we often used sparse direct solvers [4], [5], [6] or Krylov subspace methods with multi-level preconditioners [1], [2], [7], [8]. Sparse direct solvers require a large amount of memory to store the factor of the matrix $\mathbf{K} - \sigma\mathbf{M}$ thus their usage is limited due to limited amount of physical memory available on the computers. For the grid-based multi-level precondtioners [1], [2], [8], discretized vectors have to be projected from one mesh to another in the processes of restriction and prolongation. In addition, in performing time-domain analysis of the cavities

*Corresponding email: liequan@slac.stanford.edu

Work supported in part by US Department of Energy contract DE−AC02−76SF00515

with an eigen-mode as ambient load, the eigen-mode that is often computed with a different mesh needs to be projected to the mesh used for time-domain analysis. Finally, the projected eigenvector can also serve as a initial guess for the eigenvector solution of the dense mesh in eigenpair refinement.

One way for projecting a discretized vector $\mathbf{x}^a$ on mesh *a* to mesh *b* is to interpolate it on the mesh *b*. This can be viewed as solving the following linear system.

$$\mathbf{M}^b\mathbf{x}^b = \mathbf{b}^b \tag{9}$$

$$where \quad \mathbf{b}^b_j = \left(\sum_i x^a \overrightarrow{\mathbf{N}}^a_i, \overrightarrow{\mathbf{N}}^b_j\right)^b \tag{10}$$

If we interpret the discretized vector $\mathbf{x}$ as an electric field representation through Eq (2), we minimize the error of the electric fields meanwhile we have no control on the error of the magnetic fields. As matter of fact, the projected magnetic fields (or the curl of the discretized vector) often have unacceptably large errors. This will be further illustrated in Sections IV and V through examples.

## III. Method and Discussion

Let us consider the following quantity and its discretization using Eq (2) on mesh *a* or mesh *b* :

$$\overrightarrow{\mathbf{F}} \equiv \varepsilon\overrightarrow{\mathbf{E}} + \alpha\nabla\times\left(\frac{1}{\mu}\nabla\times\overrightarrow{\mathbf{E}}\right) = \varepsilon\sum_i x_i\overrightarrow{\mathbf{N}}_i + \alpha\nabla\times\left(\frac{1}{\mu}\nabla\times\sum_i x_i\overrightarrow{\mathbf{N}}_i\right) \tag{11}$$

where $\alpha$ is a constant to be specified. With the weighted residual method [9], we can use a set of weight fucntions $\overrightarrow{\mathbf{w}}_j$ to minimize the residual, $\overrightarrow{\mathbf{R}} \equiv \overrightarrow{\mathbf{F}}^b - \overrightarrow{\mathbf{F}}^a$, on mesh *b* over the domain through an inner product.

$$\left(\overrightarrow{\mathbf{w}}_j, \overrightarrow{\mathbf{F}}^b - \overrightarrow{\mathbf{F}}^a\right) = 0 \tag{12}$$

Let us choose $\overrightarrow{\mathbf{N}}^b_j$ to the the weight function $\overrightarrow{\mathbf{w}}_j$, i.e., use the Galerkin method. And we expand the above equation with (11) and get:

$$\left(\overrightarrow{\mathbf{N}}^b_j, \varepsilon\sum_i x^b_i\overrightarrow{\mathbf{N}}^b_i + \alpha\nabla\times\left(\frac{1}{\mu}\nabla\times\sum_i x^b_i\overrightarrow{\mathbf{N}}^b_i\right)\right) = \left(\overrightarrow{\mathbf{N}}^b_j, \varepsilon\sum_i x^a_i\overrightarrow{\mathbf{N}}^a_i + \alpha\nabla\times\left(\frac{1}{\mu}\nabla\times\sum_i x^a_i\overrightarrow{\mathbf{N}}^a_i\right)\right) \tag{13}$$

With integration by parts and appling proper boundary conditions, we get the following linear system:

$$(\mathbf{M}+\alpha\mathbf{K})\,\mathbf{x}^b = \left(\overrightarrow{\mathbf{N}}^b_j, \varepsilon\sum_i x^a_i\overrightarrow{\mathbf{N}}^a_i\right) + \alpha\left(\nabla\times\overrightarrow{\mathbf{N}}^b_j, \frac{1}{\mu}\sum_i x^a_i\nabla\times\overrightarrow{\mathbf{N}}^a_i\right) \tag{14}$$

As long as $\alpha$ is a non-negative number, the matrix $\mathbf{M}+\alpha\mathbf{K}$ is sysmmetric postive definite because $\mathbf{M}$ is sysmmetric postive definite and $\mathbf{K}$ is sysmmetric postive semi-definite. Thus, Eq (14) is much easier to solve than the shifted linear system Eq (8) from the eigenvalue computation. Eq (14) can be viewed as a projection of the vector $\mathbf{x}^a$ on mesh *a* to mesh *b*. The solution of it $\mathbf{x}^b$ is the discretized repsentation of $\mathbf{x}^a$ on mesh *b*.

The choice of the parameter $\alpha$ is critical. If $\alpha$ is zero, Eq (14) becomes Eq (9) and both projection methods are the same. Now let us rearrange terms in the residual $\overrightarrow{\mathbf{R}}$ as follows:

$$\begin{aligned}\overrightarrow{\mathbf{R}} &= \varepsilon\overrightarrow{\mathbf{E}}^b + \alpha\nabla\times\left(\frac{1}{\mu}\nabla\times\overrightarrow{\mathbf{E}}^b\right) - \varepsilon\overrightarrow{\mathbf{E}}^a - \alpha\nabla\times\left(\frac{1}{\mu}\nabla\times\overrightarrow{\mathbf{E}}^a\right)\\ &= \varepsilon(\overrightarrow{\mathbf{E}}^b - \overrightarrow{\mathbf{E}}^a) + \alpha\left(\nabla\times\left(\frac{1}{\mu}\nabla\times\overrightarrow{\mathbf{E}}^b\right) - \nabla\times\left(\frac{1}{\mu}\nabla\times\overrightarrow{\mathbf{E}}^a\right)\right)\end{aligned}$$

Namely, the residual $\overrightarrow{\mathbf{R}}$ have two contributing terms, one from the $\varepsilon\overrightarrow{\mathbf{E}}$ and the other from $\nabla\times\left(\frac{1}{\mu}\nabla\times\overrightarrow{\mathbf{E}}\right)$. An optimal choice of the parameter $\alpha$ is to balance those two contributing terms. Namely,

$$\left|\varepsilon(\overrightarrow{\mathbf{E}}^b - \overrightarrow{\mathbf{E}}^a)\right| = \alpha\left|\nabla\times\left(\frac{1}{\mu}\nabla\times\overrightarrow{\mathbf{E}}^b\right) - \nabla\times\left(\frac{1}{\mu}\nabla\times\overrightarrow{\mathbf{E}}^a\right)\right|$$

If an eigenvector is in the projection, we can use Eq (1) and take the difference between the two meshes and compare it with the above equation. It is clear that the optimal value of the parameter $\alpha$ is equal to $\frac{1}{k^2}$. If $\alpha$ is smaller than $\frac{1}{k^2}$, the contribution to the residual from the magnetic fields (or the curl of the electric fields) is larger than that of the electric fields. This means the error of magnetic fields can be larger after the minimization of the residual, and vice versa.

## IV. Project Analytical Fields

In this section, we take a rectangular waveguide structure with $a = 0.04m$ width, $b = 0.02m$ height, and $c = 0.08m$ length as a modeling domain. We project the following analytical fields to the two meshes for the rectangular waveguide:

$$\begin{aligned}\overrightarrow{\mathbf{E}}_x &= -\frac{\beta}{h^2}\frac{\pi}{a}cos(\frac{\pi x}{a})sin(\frac{\pi y}{b}),\\ \overrightarrow{\mathbf{E}}_y &= -\frac{\beta}{h^2}\frac{\pi}{b}sin(\frac{\pi x}{a})cos(\frac{\pi y}{b}),\\ \overrightarrow{\mathbf{E}}_z &= sin(\frac{\pi x}{a})sin(\frac{\pi y}{b}),\\ (\nabla\times\overrightarrow{\mathbf{E}})_x &= \frac{\pi}{b}sin(\frac{\pi x}{a})cos(\frac{\pi y}{b}),\\ (\nabla\times\overrightarrow{\mathbf{E}})_x &= -\frac{\pi}{a}cos(\frac{\pi x}{a})sin(\frac{\pi y}{b}),\\ (\nabla\times\overrightarrow{\mathbf{E}})_z &= 0\\ where \quad h^2 &\equiv \frac{\pi^2}{a^2} + \frac{\pi^2}{b^2} \quad and \quad \beta \equiv \sqrt{k^2 - h^2}\end{aligned}$$

One mesh has its size of $0.002m$ and the other $0.0018m$. We choose the *k* so that its corresponding frequency is 10GHz. In order to compare with the two project methods, we calculated the electric fields and magnetic fields along a line cross the waveguide ($z$ from 0 to $c$) at a quarter of width ($x = \frac{1}{4}a$) and height ($y = \frac{1}{4}b$).

The subfigures in the first column of Figure IV show the relative errors of projected electric fields and those in the second column show the relative errors of projected magnetic fields. In the first row, the analytical fields are projected onto mesh 1 with the project method described in Eq ( refeq:oldproj). The error of the magnetic fields is signficantly larger than that of the electric fields. In the second row, two projection are

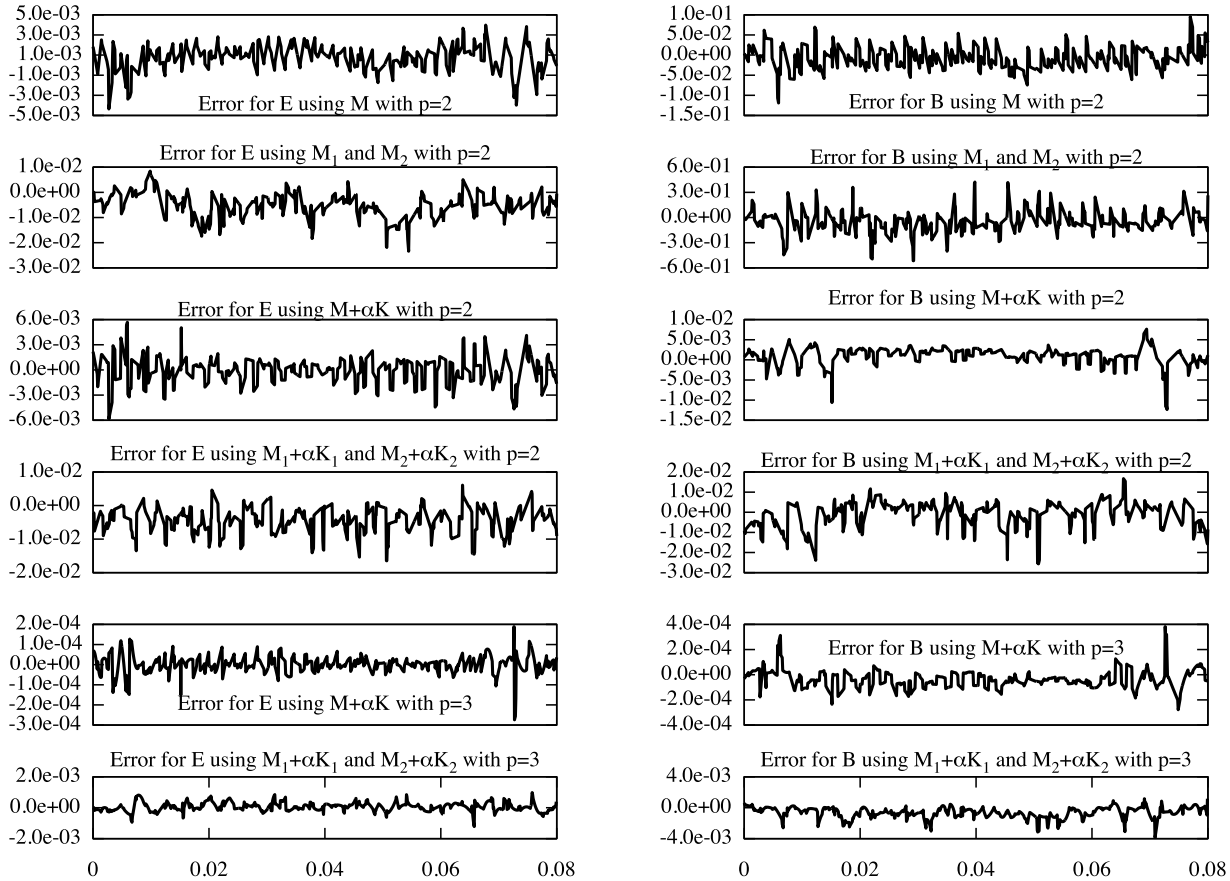


Fig. 1. The relative errors of the projected electric and magnetic fields with different projection methods.

executed, using the method described in Eq(9). The analytical fields are first projected on the mesh 1. The projected fields are again projected to mesh 2. As shown in the figures, the error of electric fields is comparable to that in the first row. However, the error of magnetic fields is signigicantly larger. In the row 3 and 4, we repeated the experiements as did in the row 1 and 2 except that we uses the projection method described in Eq (14). It is clear that the errors of the electric fields keep the comparable as those in the row 1 and 2 while the errors of the magnetic fields is signficantly better than those in the row 1 and 2. In the row 5 and 6, we repeated the experiements as did in the row 3 and 4 except that we use the finite-element order to be 3 instead of 2.

## V. Project an Eigenvector

In this section, we use a cell for the Damped Detune Structure (DDS) designed at SLAC [10] as an example for projecting eigenvectors from one mesh to another. Figure 2(a) shows one-eighth of the geometry of the cell. The rest of pictures in Figure 2 shows four meshes we used in the projection.

In this example, we first computed the eigenpair of the accelerating mode using Omega3P [11] with Mesh 1, 2, and 3, respectively. Then we project the computed eigenvector on

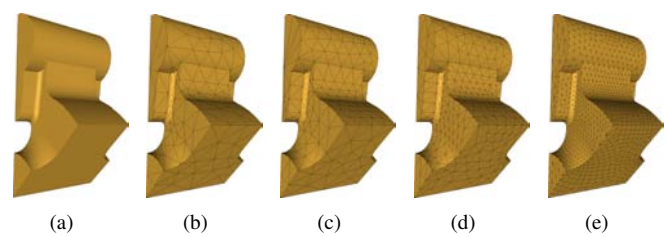


Fig. 2. (a) the CAD model of a cell for the Damped Detune Structure (DDS) for eigen-mode analysis. Only one-eighth of the geomery is shown. (b) Mesh 1 with 913 elements. (c) Mesh 2 with 1278 elements. (d) Mesh 3 with 3256 elements. (e) Mesh 4 with 19788 elements.

to Mesh 4 with $\mathbf{M}$ or with $\mathbf{M} + \alpha\mathbf{K}$ where $\alpha$ is equal to $\frac{1}{k^2}$. As a comparison, we also computed the eigenpair using Mesh 4, which is regarded as the most accurate solution since it is computed from a mesh with considerably more number of elements. To quantify and compare the errors of two project methods, we choose a line parallel to beam but offset from center and plot electric field parallel to the beam axis and one component of the magnetic fields on the line. Figure 3(a) plots the electric fields computed with Mesh 1 and 4 and the ones projected from Mesh 1 to Mesh 4 with the two different methods. Figure 3(b) plots the magnetic fields computed with

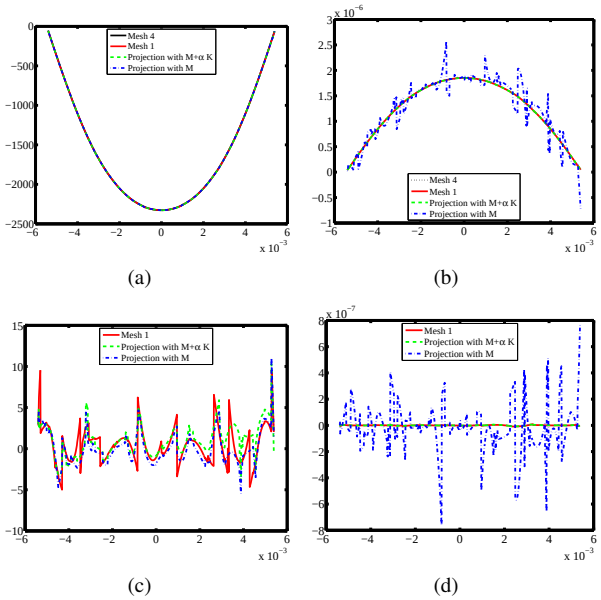


Fig. 3. (a) The electric fields computed with direct finite-element simulation using Mesh 1 and 4 and the electric fields projected from Mesh 1 to Mesh 4. (b) The magnetic fields. (c) The errors of the electric fields. (d) The errors of the magnetic fields.

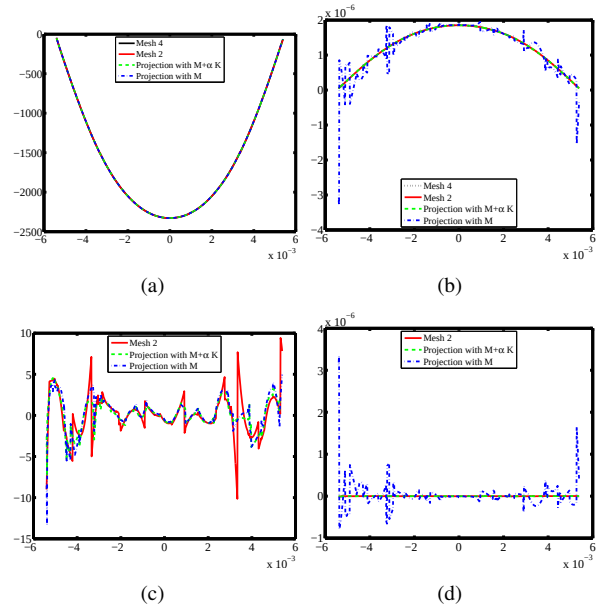


Fig. 4. (a) The electric fields computed with direct finite-element simulation using Mesh 2 and 4 and the electric fields projected from Mesh 2 to Mesh 4. (b) The magnetic fields. (c) The errors of the electric fields. (d) The errors of the magnetic fields.

Mesh 1 and 4 and the ones projected from Mesh 1 to Mesh 4 with the two different methods. Figure 3(c) plots the errors of the electric fields computed with Mesh 1 and projected from Mesh 1 to Mesh 4 with the two different methods. Note that the errors are computed with respect to the electric field computed with Mesh 4. Similary, Figure 3(d) plots the errors of the magnetic fields computed with Mesh 1 and projected from Mesh 1 to Mesh 4 with the two different methods. Figure 3(b) and 3(d) clearly indicate that the projection with $\mathbf{M}$ yields big erors for magnetic fields even though it gives a good fit for electric fields. With the projecttion method shown in Eq (14), the errors of both electric fields and magnetic fields are well controlled. In addition, the projection does not degrade the quality of the fields as the errors of the fields from direct computation and those from the projection are comparable. Figure 4 and Figure 5, plotting the similiar electric and magnetic fields and their errors but with different meshes, show the consistent results.

In solving the eigenvalue problem shown in Eq (3), we always M-orthogonalize the computed eigenvectors. Namely, make $\mathbf{x}^T\mathbf{M}\mathbf{x} = 1$. Therefore, the residual $\mathcal{R}$ defined as follows is a good measure for how accurate an appromixate eigenpair ($k^2$, $\mathbf{x}$) is. Note that the residual of a numerical eigenpair is often $10^{-15}$ or less. Table I shows the residuals of the projected eigenpairs with different meshes.

$$\mathcal{R} \equiv \left| 1 - \frac{1}{k^2}\mathbf{x}^T\mathbf{K}\mathbf{x} \right| \tag{15}$$

## VI. Summary

We proposed a new method for projecting discretized electromagnetic fields on one unstructured grid to another grid. We used two examples for studying the errors of different projection methods. The analysis shows that the new method is very effective on balancing both the error of the electric field and that of the magnetic field.

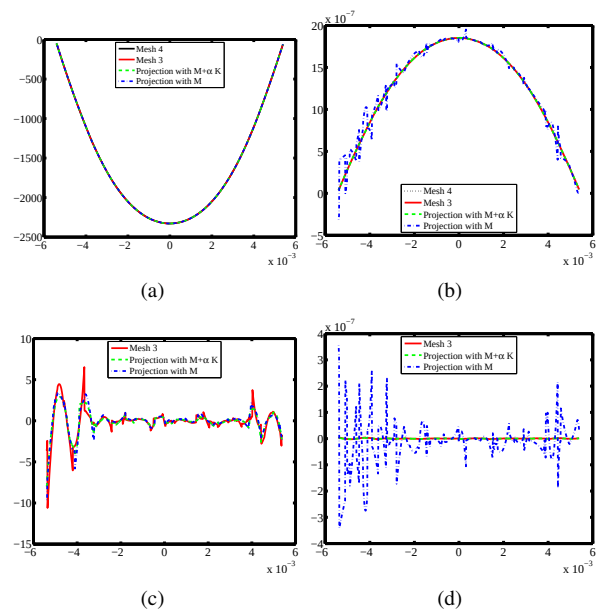


Fig. 5. (a) The electric fields computed with direct finite-element simulation using Mesh 3 and 4 and the electric fields projected from Mesh 3 to Mesh 4. (b) The magnetic fields. (c) The errors of the electric fields. (d) The errors of the magnetic fields.

## Acknowledgment

This work is supported by the U.S. Department of Energy under contract number DE-AC02 -76SF00515. Part of the work used resources of the National Center for Computational Sciences at Oak Ridge National Laboratory and resources of

TABLE I
THE RESIDUAL $\mathcal{R}$ OF THE EIGENPAIRS FOR THE DDS CELL PROJECTED FROM DIFFERENT INITIAL MESHES TO A MESH WITH 19788 ELEMENTS.

| Mesh | Number of Elements | $\mathcal{R}$ using $\mathbf{M} + \alpha\mathbf{K}$ | $\mathcal{R}$ using $\mathbf{M}$ |
|---|---|---|---|
| 1 | 913 | 0.00022 | 8.8 |
| 2 | 1278 | $4.8\times10^{-5}$ | 0.72 |
| 3 | 3256 | $5.5x10^{-6}$ | 0.020 |

the National Energy Research Scientific Computing Center, which are supported by the Office of Science of the Department of Energy under Contract DE-AC05-00OR22725 and DE-AC02-05CH11231, respectively.

## REFERENCES

[1] Y. Zhu and A. C. Cangellaris, Eds., *Multigrid Finite Element Methods for Electromagnetic Field Modeling*. Wiley-IEEE Press, 2006.
[2] R. S. Tuminaro, C. H. Tong, J. Shadid, K. Devine, and D. Day, "On a multilevel preconditioning module for unstructured mesh krylov solvers: Two-level schwarz," *Communications in numerical methods in engineering*, vol. 18, no. 6, pp. 383–389, 2002.
[3] D.-K. Sun, J.-F. Lee, and Z. Cendes, "Construction of nearly orthogonal nedelec bases for rapid convergence with multilevel preconditioned solvers," *SIAM J. SCI. COMPUT*, vol. 23, no. 4, pp. 1053–1076, 2001.
[4] A. Gupta, G. Karypis, and V. Kumar, "A highly scalable parallel algorithm for sparse matrix factorization," *IEEE Transactions on Parallel and Distributed Systems*, vol. 8, no. 5, pp. 502–520, May 1997.
[5] P. Amestoy, I. Duff, J.-Y. LÉxcellent, and J. Koster, "A fully asynchronous multifrontal solver using distributed dynamic scheduling," *SIAM Journal on Matrix Analysis and Applications*, vol. 23, no. 1, pp. 15–41, 2001.
[6] X. S. Li and J. W. Demmel, "SuperLU_DIST: A scalable distributed-memory sparse direct solver for unsymmetric linear systems," *ACM Trans. Mathematical Software*, vol. 29, no. 2, pp. 110–140, June 2003.
[7] L.-Q. Lee, L. Ge, M. Kowalski, Z. Li, C.-K. Ng, G. Schussman, M. Wolf, and K. Ko, "Solving large sparse linear systems in end-to-end accelerator structure simulations," in *Proceedings of the 18th International Parallel and Distributed Processing Symposium*, Santa Fe, New Mexico, April 2004.
[8] L.-Q. Lee and et al, "Computational science research in support of petascale electromagnetic modeling," in *Proceedings of SciDAC 2008 Conference*, Seattle, Washington, 2008.
[9] P. Seshu, *Finite Element Analysis*. Prentice Hall of India, 2004.
[10] Z. Li and et al, "X-band linear collider r&d in accelerating structures through advanced computing," in *Proceedings of EPAC 2004*, Lucerne, Switzerland, 2004.
[11] L.-Q. Lee and et al, "Omega3P: A parallel finite-element eigen-mode analysis tool for RF cavities," Stanford Linear Accelerator Center, Tech. Rep., 2008, sLAC-PUB-XXX.